



# An engineered tryptophan zipper-type peptide as a molecular recognition scaffold

Zihao Cheng<sup>‡</sup> and Robert E. Campbell\*

In an effort to develop a structured peptide scaffold that lacks a disulfide bond and is thus suitable for molecular recognition applications in the reducing environment of the cytosol, we investigated engineered versions of the trpzip class of  $\beta$ -hairpin peptides. We have previously shown that even most highly folded members of the trpzip class (i.e. the 16mer peptide HP5W4) are substantially destabilized by the introduction of mutations in the turn region and therefore not an ideal peptide scaffold. To address this issue, we used a FRET-based live cell screening system to identify extended trpzip-type peptides with additional stabilizing interactions. One of the most promising of these extended trpzip-type variants is the 24mer xxtz1-peptide with the sequence KAWTHDWTWNPATGKWTWLWRKNK. A phage display library of this peptide with randomization of six residues with side chains directed towards one face of the hairpin was constructed and panned against immobilized streptavidin. We have also explored the use of xxtz1-peptide for the presentation of an unstructured peptide 'loop' inserted into the turn region. Although NMR analysis provided no direct evidence for structure in the xxtz1-peptide with the loop insertion, we did attempt to use this construct as a scaffold for phage display of randomized peptide libraries. Panning of the resulting libraries against streptavidin resulted in the identification of peptide sequences with submicromolar affinities. Interestingly, substitution of key residues in the hairpin-derived portion of the peptide resulted in a 400-fold decrease in  $K_d$ , suggesting that the hairpin-derived portion plays an important role in preorganization of the loop region for molecular recognition. Copyright © 2009 European Peptide Society and John Wiley & Sons, Ltd.

Supporting information may be found in the online version of this article

**Keywords:** fluorescence; protein engineering; phage display; structured peptides

## Introduction

Proteins and peptides capable of specific molecular recognition in the reducing environment of a cell's interior are valued as research reagents or potential therapeutic leads [1–3]. Antibodies are, ostensibly, the protein family of choice for most biological molecular recognition applications. These versatile molecular recognition reagents can be readily generated either by traditional immunization or hybridoma techniques [4,5] and provide researchers with high specificity and high affinity research tools. However, their use in live cell intracellular applications is generally limited by the technical challenge of getting these large proteins across the cell membrane. For research applications (as opposed to therapeutic applications), this problem can be circumvented by recombinant expression of genes encoding the heavy and light chains of the antibody in the target cell. However, this approach is limited by the poor folding efficiency of antibodies in the reducing environment of the cytosol due to an inability to form the multiple disulfide bonds that are critical for their stability [6]. Much work has been invested in the development of recombinant engineered antibody fragments [7] that can be expressed in living cells and retain the binding specificity and affinity of the intact antibody from which they were derived [8,9]. An alternative approach is to engineer nonimmunoglobulin proteins or peptides to have molecular recognition functions that are not dependent on the formation of a disulfide bond [2,10,11].

The nonimmunoglobulin domain proteins best suited for conversion into molecular recognition domains have been referred

to as 'generic protein scaffolds': proteins that have effectively separated the parts of their tertiary structures that confer structural stability and the parts that confer the molecular recognition function [12]. A desirable feature of a generic protein scaffold intended for intracellular applications is a relatively small size, which is generally thought to reduce nonspecific binding and allow access to epitopes that are sterically occluded from larger domains. Among the smallest validated generic protein scaffolds are zinc fingers [13,14] and the Trp-cage motif [15] at just 26 and 20 residues, respectively. Despite their small size, these peptides meet the basic criteria of a generic proteins scaffold because the parts of the structures that confer structural stability (i.e. the Cys<sub>2</sub>His<sub>2</sub> coordination of a zinc ion in a zinc finger and the buried tryptophan of a Trp-cage) are independent of the part the structure used for the molecular recognition function (i.e. the five contiguous residues on

\* Correspondence to: Robert E. Campbell, Department of Chemistry, University of Alberta, Edmonton, Alberta, Canada T6G2G2.  
E-mail: robert.e.campbell@ualberta.ca

Department of Chemistry, University of Alberta, Edmonton, Alberta, Canada T6G 2G2

‡ Present address: Gilead Alberta ULC, 1021 Hayter Road, Edmonton, Alberta, Canada T6S1A1.

**Abbreviations used:** CFP, cyan fluorescent protein; FRET, fluorescence resonance energy transfer; SPR, surface plasmon resonance; trpzip, tryptophan zipper; YFP, yellow fluorescent protein;  $\langle \cos^2 \theta \rangle$ , orientation factor for energy transfer.

the face of an  $\alpha$ -helix in a zinc finger and the seven solvent-exposed residues of the Trp-cage). As with proteins, a highly folded and preorganized structure will minimize the entropic cost of a peptide adopting the conformation necessary for target binding and may thereby lead to higher affinity reagents.

Trpzip  $\beta$ -hairpin peptides [16] are another promising candidate for a small generic protein scaffold. They are only 16 to 20 amino acids in length, soluble, monomeric, and form highly stable  $\beta$ -hairpins in aqueous solution [16]. One of the most stable trpzip-type peptides reported to date is a 16mer known as **HP5W4** (Table 1) [17]. Much of the fold stability of these peptides arises from two pairs of tightly packed cross-strand Trp–Trp pairs on one

face of the  $\beta$ -hairpin (Figure 1) [16]. Accordingly, we reasoned that it might be possible to find a particularly stable variant that would retain the  $\beta$ -sheet structure upon randomization of a subset of its amino acids or even insertion of additional randomized residues in the turn region.

A  $\beta$ -hairpin with additional residues inserted into the turn region is an intriguing minimal scaffold for the intracellular display of constrained peptides [18,19]. Such a structure has been previously proposed for an engineered peptide composed of two copies of an antiparallel dimerizing peptide derived from neuropeptide head activator [20], which presumably forms a two-stranded  $\beta$ -sheet (the stem), flanking an unstructured sequence

**Table 1.** Proteins and peptides investigated in the this work

Protein name	Peptide name	Peptide sequence <sup>a</sup>
<b>tz1</b>	<b>HP5W4</b>	KK---WTWNP-----TGKWTW----QE
<b>xtz1</b>	<b>xtz1</b> -peptide	KAWT--WTWNP-----TGKWTW--RKNE
<b>xxtz0.5</b>	NA <sup>b</sup>	KAWTHDWTWNP-----TGKWTWLRKNE
<b>xxtz1</b>	<b>xxtz1</b> -peptide	KAWTHDWTWNP-----TGKWTWLRKKNK
<b>tz1/loop</b>	NA	KK---WTWNPGGGGGGGGKWTW----QE
<b>xtz1/loop</b>	NA	KAWT--WTWNPGGGGGGGGKWTW--RKNE
<b>xxtz0.5/loop</b>	NA	KAWTHDWTWNPGGGGGGGGKWTWLRKNE
<b>xxtz1/loop</b>	NA	KAWTHDWTWNPGGGGGGGGKWTWLRKKNK
NA	<b>xxtz1/loop</b> -peptide	KAWTHDWTWNPSSSSSGGKWTWLRKKNK

<sup>a</sup> The 'protein' is the indicated peptide sequence with CFP appended to its N-terminus and YFP appended to its C-terminus. The 'peptide' is the indicated sequence with few or no additional amino acids appended to its N- and C-termini. The **xxtz1**-peptide has GAQ appended to its N-terminus and GT appended to its C-terminus.

<sup>b</sup> Not applicable, construct was not made.

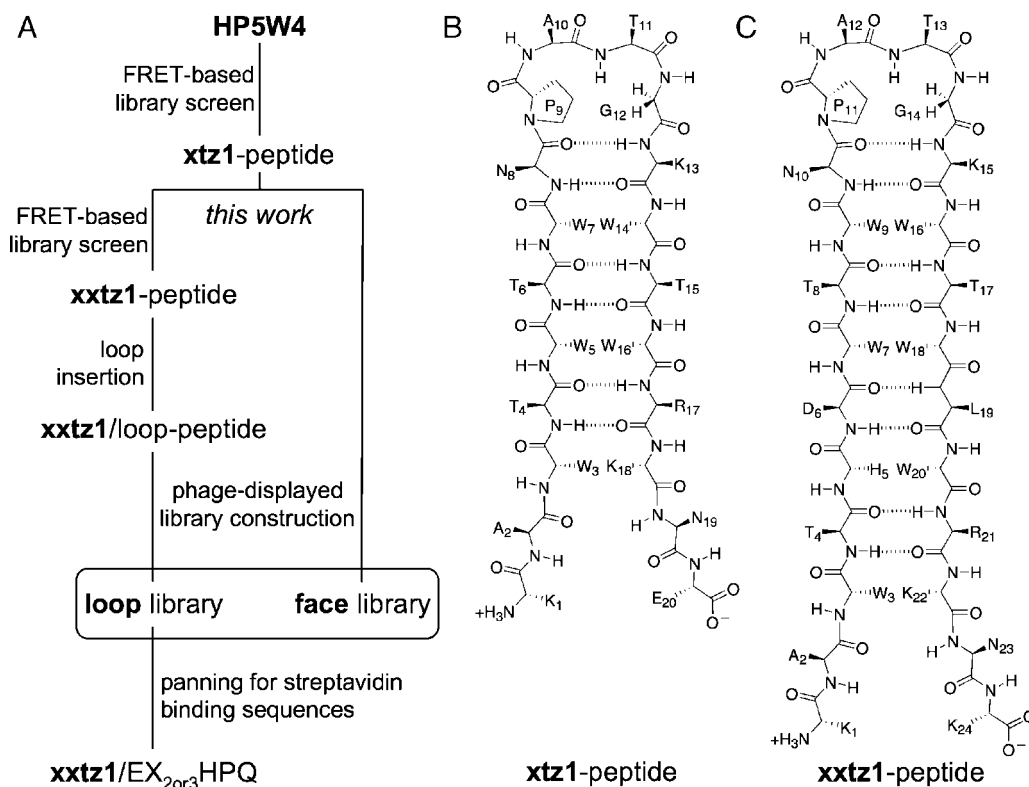


**Figure 1.** Schematic representation of the overall strategy and specific peptide scaffolds investigated in this work. (A) Flowchart outlining the relationship of the various peptides and peptide libraries investigated in this work. (B) Schematic representation of the **xtz1**-peptide structure [24]. (C) Proposed structure of the **xxtz1**-peptide based on analogy with the experimentally determined structure of the **xtz1**-peptide.

of randomized residues (the loop) [19]. Although this design is compelling, evidence supporting the existence of the stem-loop peptide structure is inconclusive. Indeed, an NMR study by Lai and Gellman [21] provided evidence that even with a strongly  $\beta$ -hairpin promoting D-Pro-Gly sequence in place of the unstructured loop, the SKVILF stem structure is only moderately stable. A recent CD study by Anderson and colleagues [22] led the authors to conclude that tandem copies of EFLIVKS (the retro sequence of neuropeptide head activator) can serve to tether together the ends of an intervening 18 residue unstructured loop. It occurred to us that, regardless of whether the neuropeptide head activator (or its retro sequence) is able to self dimerize or not, there may exist other peptide sequences that are more effective at forming the stem portion of the stem-loop peptide structure. Furthermore, peptide sequences that adopt extremely stable  $\beta$ -hairpin structures might be particularly amenable to conversion into stem-loop structures by replacement of their turn sequences with longer sequences of randomized residues.

We recently developed a method for rapid high-throughput screening of thousands of peptide sequences to find ones that are highly structured in live cells [23–25]. This system relies on fluorescence imaging of plates of *Escherichia coli* colonies where each colony expresses a single protein construct composed of a CFP and a YFP flanking an intermediary peptide sequence [23]. Highly structured and compacted peptide sequences bring the CFP and YFP proteins into closer proximity, or a more optimal orientation, which results in more efficient FRET. Higher FRET efficiency is manifested as a ratiometric change in fluorescence intensity that is simultaneously measured for hundreds of bacterial colonies using quantitative image acquisition and processing. Colonies exhibiting higher FRET ratios are picked and their plasmid DNA isolated. DNA sequencing shows the peptide sequence responsible for bringing the two fluorescent proteins into an arrangement that is more conducive to FRET.

In previous work, we had applied our *in vivo* screening method to the **HP5W4** peptide in an effort to engineer additional stabilizing interactions into this  $\beta$ -hairpin. Our strategy involved extending the sequence by two randomized residues in each strand of the  $\beta$ -hairpin. Iterative library screening resulted in the identification of the **xtz1** protein that harbors the 20mer **xtz1**-peptide (Figure 1 and Table 1), which has an additional cross-strand lysine-tryptophan cation- $\pi$  interaction relative to **HP5W4** [24]. We now report our continued efforts to engineer additional stabilizing interactions into these trpzip-type peptides through the use of our *in vivo* screening approach. We have further extended the  $\beta$ -hairpin sequence to 24 residues with exhaustive screening of all possible amino acid combinations at each new pair of cross-strand residues. To investigate the potential of our most promising 24mer peptide for use as a generic peptide scaffold, we have used phage display-based screening [26] to explore the use of this minimal and disulfide bond-free scaffold for the identification of peptide ligands.

## Materials and Methods

### General Methods and Materials

All synthetic DNA oligonucleotides were purchased from Integrated DNA Technologies. PCR products and products of restriction digestion were routinely purified using the QIAquick PCR purification kit or QIAEX II gel extraction kit (Qiagen). Plasmids were purified using GeneJet plasmid miniprep kit (Fermentas) according to the manufacturer's protocol. Restriction enzymes and Taq DNA

polymerase were purchased from New England Biolabs and used with the supplied buffers. Ligations were performed using T4 DNA ligase (Invitrogen) according to the manufacturer's instructions. The composition of the peptide portions of all FRET constructs was determined by dye terminator cycle sequencing using the DYEnamic ET kit (Amersham Biosciences) and a forward primer (5'-CCC TCG TGA CCA CCC TGA CCT GG-3') that anneals to the chromophore region of the gene encoding CFP. The primer used for sequencing of the displayed portion of phagemid pComb3ZC was 5'-AGG CTT TAC ACT TTA TGC TTC CGG C-3'. All sequencing reactions were analyzed at the University of Alberta Molecular Biology Service Unit. Protein samples for *in vitro* spectral characterization experiments were first dialyzed into 50 mM Tris, pH 7.5. The protein referred to as YFP is the Ala206Lys [27] variant of citrine [28]. The protein referred to as CFP is a variant of cerulean [29] that has been used in prior studies [23]. All filters used in imaging were purchased from Chroma Technology.

### FRET-based Library Screening

The CFP-peptide-YFP libraries were expressed using the previously described vector pZC1 [23] derived from pBAD/His B (Invitrogen) which contains the arabinose-dependent *araBAD* promoter. The pZC1 vector can be used to express genes encoding proteins of the general structure  $N_{\text{term}}\text{-His}_6\text{-EK-CFP}(1\text{--}230)\text{-TSGAQ-peptide-GTSAE-YFP}(5\text{--}238)\text{-C}_{\text{term}}$ , where *His*<sub>6</sub> is six consecutive histidine residues that facilitate metal affinity purification [30], and *EK* is the recognition sequence for the protease enterokinase. The DNA encoding the TSGAQ amino acid sequence (ACT AGT GGA GCT CAG) contains both a *Spe*I and a *Sac*I restriction site. The DNA encoding the GTSAE sequence (GGT ACC TCT GCA GAG) contains both a *Kpn*I and a *Pst*I restriction site. Preparation of the peptide libraries for FRET-based screening is described in Supplementary Methods (Supporting Information).

The system for imaging of the fluorescence of bacterial colonies has previously been described in some detail [23]. For a given Petri dish, fluorescence images were acquired in three channels that correspond to CFP donor (excitation 436/20 nm, emission 480/40 nm), FRET (excitation 436/20 nm, emission 535/30 nm), and YFP acceptor (excitation 500/20 nm, emission 535/30 nm). An Image Pro plus (Media Cybernetics) macro was used for automatic identification of colonies within digital images, summing of the pixel intensities in each of three channels for each colony, and exporting the data to a spreadsheet. For each colony, the emission ratio was calculated by dividing the intensity in the FRET channel by the intensity in the CFP donor channel. Colonies that had the highest emission ratios and the highest brightness in the YFP acceptor channel were picked using a sterile tip and used to inoculate LB liquid media (5 ml) supplemented with ampicillin (0.1 mg/ml) and arabinose (0.2% w/v). Cultures were grown overnight at 37 °C with shaking at 225 rpm. The following day, protein was extracted from 1 ml of each culture using B-per II (Pierce) and emission spectra acquired using a Sapphire2 fluorescence 96-well platereader equipped with monochromators (Tecan). Plasmid DNA was isolated and sequenced for those clones that exhibited the highest FRET emission ratios.

### Protein Purification

A typical protein purification procedure started with the inoculation of 1 l LB media containing ampicillin (0.1 mg/ml) and arabinose (0.2% w/v) with a single colony of *E. coli* DH10B previously transformed with the expression plasmid. Cultures were

grown overnight at 37 °C with shaking at 225 rpm, cooled to 4 °C on ice, and harvested by centrifugation (10 min, 5000 rpm). The cell pellet was resuspended in PBS buffer (137 mM NaCl, 2.7 mM KCl, 10 mM phosphate, pH 7.4) and the cells were lysed by a single passage through a French Press (Thermo Electron). Insoluble cell debris was pelleted by centrifugation at 4 °C (10 min, 10 000 rpm) and 1 ml of Ni-NTA resin (Qiagen) was added to the supernatant. Following 1 h of gentle mixing at 4 °C, the supernatant was loaded onto a 6 ml polypropylene column, washed, and gravity eluted in 250 mM imidazole (pH 7.5) according to the manufacturer's protocol. Proteins were further purified on an AKTAdesign chromatography system (Amersham Biosciences) equipped with a Hiloal 16/60 Superdex 75 prepgrade gel filtration column that was equilibrated with 50 mM Tris pH 7.5. Isolated proteins were concentrated with a Centricon centrifugal filter YM-30 (Millipore) and stored at 4 °C.

### Peptide Production

Recombinant expression of a fusion protein in *E. coli* was used to produce the **xtz1**-peptide. We previously reported a plasmid [23] that can be used to express proteins of the general structure  $N_{\text{term}}\text{-His}_6\text{-EK-CFP}(1-230)\text{-AcTEV-AQ-peptide-GT-C}_{\text{term}}$ , where *AcTEV* is the protease substrate sequence QNLYFQG, and AQ and GT represent the amino acids encoded by the *Sac1* (GGA GCT CAG) and *Kpn1* (GGT ACC) sites, respectively. A stop codon follows the *Kpn1* site. This plasmid was digested with *Sac1* and *Kpn1* and ligated with the similarly digested DNA fragment that had been PCR amplified from pZC1/**xtz1** using the primers that had also been used for error-prone PCR. The resulting plasmid was used to transform *E. coli* and the protein product purified as described above. Following purification, the protein was treated with *AcTEV* protease (Invitrogen) to release the peptide-containing fragment [23]. To produce the **xtz1/loop**-peptide, we used SPPS on a ABI 433A peptide synthesizer (Applied Biosystems). Both the **xtz1**-peptide and the **xtz1/loop**-peptide were purified by RP chromatography on a Prosphere HP C18 300A column (Alltech Associates, Inc.) using a linear gradient of increasing acetonitrile in H<sub>2</sub>O with 0.1% TFA. The fraction containing each target peptide was lyophilized to provide a fluffy white solid (yield ~2 mg **xtz1**-peptide and ~50 mg **xtz1/loop**-peptide). MALDI-TOF-MS showed molecular weights of 3513.06 *m/z* (3513.97 *m/z* calculated) and 3446.62 *m/z* (3446.84 *m/z* calculated) for **xtz1**-peptide and **xtz1/loop**-peptide, respectively. A calculated extinction coefficient of 33 450 M<sup>-1</sup> cm<sup>-1</sup> at 280 nm was used to determine concentrations.

### Spectroscopy

Fluorescence spectra for all proteins (40 nm) were recorded on a QuantaMaster spectrofluorometer (Photon Technology International) and FRET efficiencies were determined by trypsinolysis as previously described [23]. Errors for three of more measurements were reported as standard deviation. CD spectra were obtained with 40 μm peptide in a 1 mm path length cuvette on an Olis DSM 17 CD spectrometer (Olis). <sup>1</sup>H NMR spectra of **xtz1/loop**-peptide in buffer [10 mM NaH<sub>2</sub>PO<sub>4</sub> pH 6, 10% D<sub>2</sub>O in H<sub>2</sub>O, with internal 2,2-dimethyl-2-silapentane-5-sulfonic acid (DSS) reference] were obtained with a Varian 500 MHz spectrometer with presaturation of the H<sub>2</sub>O peak. Various spectra were acquired at peptide concentrations between 0.1 and 2 mM TFE concentrations between 0% and 50%, and temperatures between 5 and 50 °C. The <sup>1</sup>H NMR

spectrum of **xtz1**-peptide was obtained with a Varian 600 MHz spectrometer as previously described [24].

### Phage Library Panning and Enrichment

Construction of the phage library is described in Supplementary Methods. All panning and enrichment were performed by following established protocols [31]. Enrichments of streptavidin-binding peptides displayed on phage were performed by panning against streptavidin magnetic beads (Invitrogen). Briefly, 20 μl of streptavidin magnetic beads were first incubated with BSA (3% w/v) in PBS for 1 h. Control panning experiments were performed under identical conditions with beads that had been preincubated with biotin. Approximately 5 × 10<sup>11</sup> phage were added to the beads and gently mixed for 1 h. The beads were washed with 10 × 1 ml PBS buffer containing 0.5% Tween20 to remove unbound and weakly bound phage. The adherent phage were then eluted with 0.1 mM biotin in PBS and added to 2 ml prepared XL1-blue *E. coli* culture and incubate at room temperature for 15 min. Pre-warmed SB medium was then added to the infected *E. coli* culture with 25 μg/ml carbenicillin and 10 μg/ml tetracycline. After 2 h of incubation at 37 °C, the VCSM13 helper phage was added. Kanamycin was added to the culture 2 h later, and the preparation of phage continued as described above. After three to four rounds of enrichment and amplification, five bacterial colonies from each library were picked and cultured. DNA sequencing was used to reveal the gene sequence that corresponded to the displayed peptide portion.

### Binding Analysis

Peptide sequences selected by phage display were PCR amplified from their purified phagemids and inserted into an appropriate plasmid for production of proteins of the general structure CFP-peptide-YFP as described in Supplementary Methods. Kinetic analysis of these proteins binding to streptavidin was performed with a Biacore X instrument at 25 °C. A streptavidin pre-coated chip (SA chip, Biocore Inc.) was used for all measurements with HEP-EP buffer (10 mM HEPES, 150 mM NaCl, pH 7.4) as the running buffer at a flow rate of 10 μl/min. To generate each sensorgram, 30 μl of freshly purified protein in HEP-EP buffer was injected. Equilibrium dissociation constants (*K<sub>d</sub>*) were calculated with BIAevaluation 4.1 (Biocore Inc.) software package which fit the data to the Langmuir 1 : 1 binding model.

The FRET-based determination of solution *K<sub>d</sub>*s for protein binding to streptavidin was performed on a Safire2 monochromator-based plate reader (Tecan). Briefly, to a solution of each purified FRET construct (50 nM) was added a buffered solution of streptavidin (Roche) to the desired final concentration. The ratio of fluorescence intensity at 530 and 480 nm (excitation at 430 nm) was recorded and plotted as a function of streptavidin concentration. The data was fit with an equilibrium binding model that assumes only that there is no binding in the initial (high FRET) state and 100% binding in the final (low FRET) state.

### Results

The names of peptides and proteins used in this work are summarized in Table 1. We use the convention that the short bolded names (e.g. **xtz1**) refer to proteins of the type CFP-peptide-YFP, where the peptide is a specific sequence of between 16 and 24

residues in length. When referring to the isolated peptide portions with no fluorescent proteins attached, we add the suffix '-peptide' (e.g. **xtz1**-peptide).

### FRET-based Screening of Libraries of Extended $\beta$ -Hairpin Peptides

In an effort to explore the possibility of further extending our previously reported 20mer **xtz1**-peptide (Table 1) [24], we created a library of peptide variants in which two additional pairs of residues, one randomized and one threonine, were genetically inserted after the 4th and 16th residues of the peptide portion of **xtz1** (Table 2). Using the numbering of the 24mer peptide (which will be used for the remainder of the manuscript unless otherwise noted), the inserted residues are at positions 5, 6, 19, and 20. A genetic library of these 400 peptide variants, with CFP fused to the N-terminus and YFP fused to the C-terminus, was expressed in *E. coli* and screened by ratiometric fluorescence imaging of colonies [23–25]. We screened several thousand colonies and, for the eight colonies exhibiting the highest YFP/CFP ratios, sequenced the section of cDNA encoding the peptide portion of the FRET construct. The sequences showed a modest preference at the randomized 5th and 20th positions for a positively charged residue (Arg or His) paired with a Trp, or seemingly any residue (Met, Lys, and Gly observed) paired with a Pro (Table 2).

We constructed a second library in which the 6th and 19th positions were randomized to all amino acids and the 5th and 20th positions were randomized to a subset of the residues most commonly selected in the first library (Table 2). Screening of this second library for high FRET variants resulted in the identification of a series of variants that exhibited a stronger preference in their amino acid sequence than had been observed in the first

library. Specifically, at the 5th and 20th positions there was strong preference for Trp residues, paired with either a positively charged residue (Lys, Arg, or His) or another Trp. At the 6th position, there was a strong preference for a charged residue (His or Asp). These observed preferences are consistent with previous work on  $\beta$ -hairpin peptides in which it was shown that diagonal cross-strand pairs of Trp with Lys or Arg engage in stabilizing cation- $\pi$  interactions [32]. The 19th position exhibited the least bias, with some apparent preference for a hydrophobic residue (Leu or Val). *In vitro* measurements of FRET efficiency for purified samples of each of the proteins showed that the sequence with the amino acid combination of His, Asp, Leu, and Trp at positions 5, 6, 19, and 20, respectively, had the highest FRET efficiency (data not shown). This protein was designated **xxtz0.5** (Table 1). The peptide portion of **xxtz0.5** was subjected to three iterative rounds of random mutagenesis by error-prone PCR and libraries of proteins were screened for high FRET efficiency. Sequencing of the variant with the highest FRET at the end of the third round showed only the Glu24Lys substitution. Presumably, in two of the rounds the highest FRET variant was identical to **xxtz0.5**. This Glu24Lys variant of **xxtz0.5** was designated **xxtz1**.

### Characterization of Extended $\beta$ -Hairpin Peptides

As shown in Table 3, *in vitro* measurements confirmed that the empirical screen for high YFP/CFP ratio *in vivo* had indeed resulted in the identification of proteins exhibiting high FRET efficiency. In going from **tz1** to **xtz1** to **xxtz1**, the FRET efficiency increased from 59% to 67.9% to 84.5%. It is important to note that as the overall length of polypeptide sequence between the two fluorescent proteins increases, the FRET efficiency is expected to decrease, all other factors being the same. For example, proteins

**Table 2.** Peptide sequences identified by FRET-based libraries screening

	Library <sup>a</sup>	Sequences identified			
		X <sup>5</sup>	X <sup>6</sup>	X <sup>19</sup>	X <sup>20</sup>
1st	K <sup>1</sup> A <sup>2</sup> W <sup>3</sup> T <sup>4</sup> X <sup>5</sup> T <sup>6</sup> W <sup>7</sup> T <sup>8</sup> W <sup>9</sup> N <sup>10</sup> P <sup>11</sup> A <sup>12</sup> T <sup>13</sup> G <sup>14</sup> K <sup>15</sup> W <sup>16</sup> T <sup>17</sup> W <sup>18</sup> T <sup>19</sup> X <sup>20</sup> R <sup>21</sup> K <sup>22</sup> N <sup>23</sup> E <sup>24</sup>	W W H M K E G			R R W P P T P
		(W/K/H/R/D/G) <sup>5</sup>	X <sup>6</sup>	X <sup>19</sup>	(W/T/S/P/R) <sup>20</sup>
2nd	K <sup>1</sup> A <sup>2</sup> W <sup>3</sup> T <sup>4</sup> (W/K/H/R/D/G) <sup>5</sup> X <sup>6</sup> W <sup>7</sup> T <sup>8</sup> W <sup>9</sup> N <sup>10</sup> P <sup>11</sup> A <sup>12</sup> T <sup>13</sup> G <sup>14</sup> K <sup>15</sup> W <sup>16</sup> T <sup>17</sup> W <sup>18</sup> X <sup>19</sup> (W/T/S/P/R) <sup>20</sup> R <sup>21</sup> K <sup>22</sup> N <sup>23</sup> E <sup>24</sup>	H W W W H K W	D H D D H G H	L T L Q L V Q	W <sup>b</sup> R W W W W W
3rd	Error-prone PCR on <b>xxtz0.5</b>		<b>xxtz0.5</b> with E24K substitution <sup>c</sup>		
4th	Error-prone PCR on <b>xxtz1</b>		No higher FRET variants identified		

<sup>a</sup> Positions marked 'X' were subject to saturation mutagenesis by using the codon 'NNK' where N = adenine (A), guanine (G), cytosine (C), or thymine (T), and K = G or T.

<sup>b</sup> This sequence was designated as **xxtz0.5**.

<sup>c</sup> This sequence was designated as **xxtz1**.

**Table 3.** FRET efficiencies for proteins with and without loop insertions

Protein	FRET efficiency (%)	Protein with loop insertion	FRET efficiency (%)
<b>tz1</b>	59.0 ± 0.7	<b>tz1/loop</b>	51.3 ± 0.5
<b>xtz1</b>	67.9 ± 1	<b>xtz1/loop</b>	65.3 ± 0.6
<b>xxtz0.5</b>	70.1 ± 1	<b>xxtz0.5/loop</b>	68.4 ± 0.6
<b>xxtz1</b>	84.5 ± 0.7	<b>xxtz1/loop</b>	74.6 ± 0.2

with unstructured polypeptide linkers of identical lengths to those of **tz1** (16 residues) and **xtz1** (20 residues) have FRET efficiencies of  $47.2 \pm 1\%$  [23] and  $44.0 \pm 0.8\%$  [25], respectively. Of course, all other factors are not the same in the **tz1/xtz1/xxtz1** series, as we have purposely selected for peptide sequences that provide the highest FRET efficiency. The high FRET efficiency measured for **xxtz1** provides qualitative support for the conclusion that the peptide portion of this protein is at least as structured at room temperature as the preceding members of the series.

To determine whether the peptide portion of **xxtz1** is highly structured when removed from the context of the fluorescent protein fusion protein, **xxtz1**-peptide was expressed and purified. A characteristic feature of the CD spectra of trpzip-type peptides is a strong negative band at approximately 215 nm and a strong positive band at approximately 230 nm [16]. These features are attributed to exciton coupling of the two pairs of closely packed indole sidechains of tryptophan [33]. The similarities of the CD spectra and the signal magnitude of the **xxtz1**-peptide in comparison with **HP5W4** and **xtz1**-peptide (Figure 2A) confirmed that the additional residues do not substantially disrupt the packing of the tryptophan indole side chains at positions 7, 9, 16, and 18. However, a slight red shift indicates possible differences in the packing of the indole moieties and a new minimum at 205 nm indicates some random coil conformation (possibly at the ends of the peptide). The CD melting curve showed that the **xxtz1**-peptide has a melting point approximately 15 °C lower than its precursor **HP5W4** (Figure 2B). Close inspection of Figure 2B showed that **HP5W4**, **xtz1**-peptide, and **xxtz1**-peptide all exhibit an effectively identical degree of melting between 5 and 20 °C. It is only at temperatures substantially higher than the screening temperature (20 °C) that differences in the peptide-fold stability manifest themselves.

### Insertion of an Unstructured Loop into a $\beta$ -Hairpin Peptide

As shown in Table 3, replacement of the Ala-Thr of the turn sequence with a Gly<sub>7</sub> loop (refer to Table 1) diminished the FRET efficiency for all four proteins. However, the FRET efficiencies remained substantially greater than that observed (or expected) for an unstructured linker of the same length. As mentioned above, CFP-YFP fusion proteins with unstructured linkers identical in length to the peptides of **tz1** and **xtz1** have FRET efficiencies of 47% and 44%, respectively. A similar analog of **xxtz0.5** and **xxtz1** was not prepared, but its FRET efficiency is certain to be less than 44% due to the increased peptide length.

To further investigate the peptide portion of the **xxtz1/loop** variant, we synthesized and purified a synthetic peptide analog (**xxtz1/loop**-peptide, Table 1). The primary difference between the **xxtz1/loop**-peptide and the peptide portion of the **xxtz1/loop** protein is that four of the seven glycine residues in the unstructured

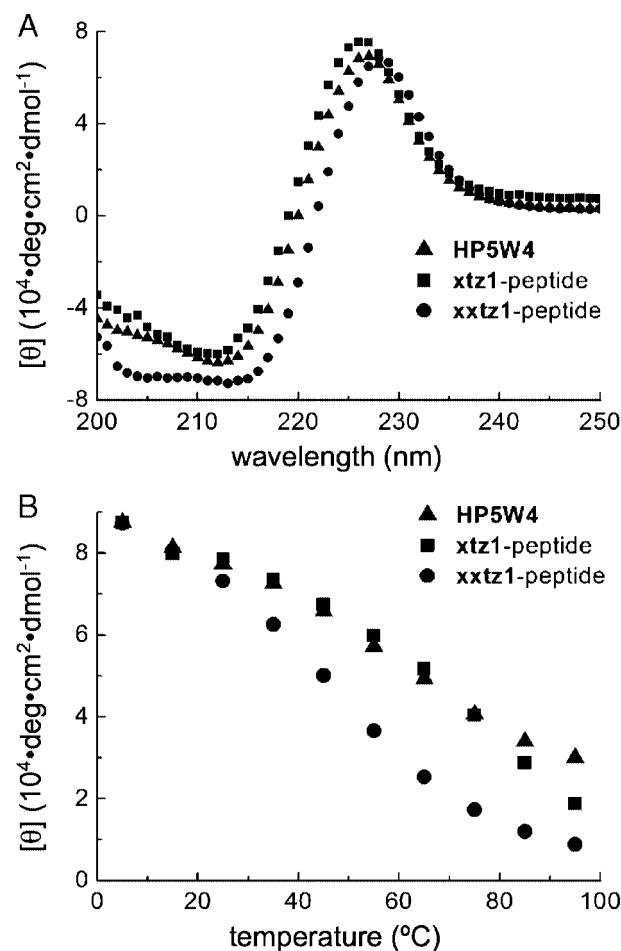


**Figure 2.** CD characterization of peptides. (A) CD spectra of identical concentrations of **HP5W4**, **xtz1**-peptide, and **xxtz1**-peptide. (B) CD melting curves at 227 nm for the three peptides represented in (A).

loop sequence have been replaced by serine to make the peptide sequence more hydrophilic and, potentially, improve its solubility. Indeed, the purified peptide was highly soluble in aqueous solution (greater than 5 mM), a characteristic that is generally associated with a highly folded trpzip-type structure [16]. However, CD analysis of **xxtz1/loop**-peptide showed only a relatively weak exciton coupling band at 230 nm and a negative band at approximately 205 nm, consistent with almost complete loss of the critical tryptophan packing interactions and increased random coil character (Figure 3).

The apparent lack of structure for the **xxtz1/loop**-peptide was confirmed by <sup>1</sup>H NMR spectroscopy (Supplementary Figure 1). At 2 mM peptide concentration, the peaks in the NMR spectrum were broad and poorly dispersed, indicating that the peptide was likely aggregated (resulting in an increased rotational correlation time) and unstructured. At concentrations of 1 mM and less, line widths were decreased but dispersion remained poor. The addition of TFE at concentrations of up to 50% resulted in further decrease in line widths and somewhat better dispersion of peaks. Coupling constants for all HN resonances fell within the range of 6–8 Hz. The overall appearance of the **xxtz1/loop**-peptide spectrum contrasts starkly with the excellent dispersion of peaks observed in the previously acquired <sup>1</sup>H NMR spectrum of **xtz1**-peptide (Supplementary Figure 1). Indeed, backbone HN resonances for residues that are present in both peptides are

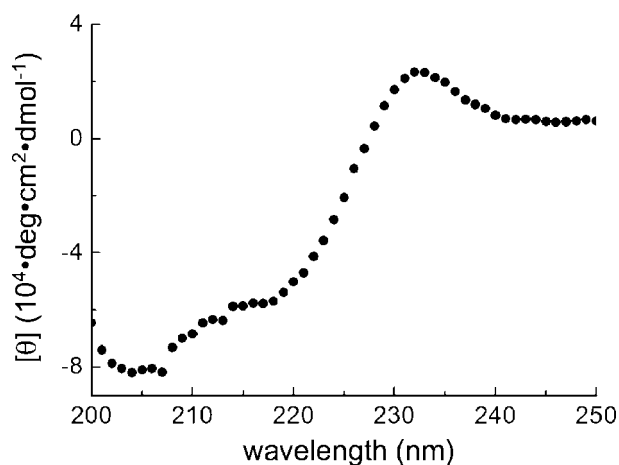


**Figure 3.** CD spectrum of **xxtz1/loop**-peptide. Experimental conditions are identical to those used in Figure 2A.

shifted substantially more upfield in **xxtz1/loop**-peptide than in **xztz1**-peptide. For example, the HN hydrogen atoms of the Trp residues of **xztz1**-peptide that align with Trp 7, 9, 16, and 18 of **xxtz1/loop**-peptide resonate at chemical shifts of 9.17, 8.78, 8.70, and 8.73 ppm, respectively. Resonances at similar chemical shifts were not observed in the **xxtz1/loop**-peptide spectra acquired at any temperature with or without TFE (up to 50%). These results indicate that this peptide does not fold into a hairpin-type structure to any appreciable degree under the conditions of the NMR experiment.

#### Phage Display with a $\beta$ -Hairpin Scaffold and a Loop Insertion Scaffold

To explore the potential of trpzip-type  $\beta$ -hairpins as scaffolds for molecular recognition, phage display libraries based on **xztz1**-peptide and **xxtz1/loop**-peptide were constructed and screened. Although the apparent lack of structure in the **xxtz1/loop**-peptide would seem to make it a poor candidate for this purpose, we found the FRET results intriguing enough to justify the attempt. The peptide libraries were displayed as fusions to a truncated version of the pIII protein of the M13 Ff filamentous bacteriophage [31] and panned with selection for streptavidin binding. The **xztz1**-peptide **face** library was constructed by genetically randomizing six amino acids that have side chains oriented towards the face of the  $\beta$ -hairpin that is opposed to the face where the tryptophan side chains are packed. Specifically, the residues at positions 4, 6, 10, 11, 15, and 17 (Figure 1 and Table 4) were randomized through the introduction of degenerate NNK codons. The **xxtz1/loop**-peptide **loop** library was generated by replacing the GSSGSSG loop with a sequence of seven randomized residues (using NNK codons) flanked by single Gly residues on either side (Table 4). Libraries of

$7 \times 10^7$  and  $4 \times 10^8$  independent clones were obtained for the **face** and **loop** libraries, respectively. Following several rounds of panning against streptavidin immobilized on magnetic beads, the phage output was observed to dramatically increase in terms of both absolute number of phage eluted as well as output relative to a control (Figure 4). The control experiments were performed identically to the selection experiments, except the immobilized streptavidin was preincubated with an excess of biotin.

It is well documented that peptides with a His-Pro-Gln (HPQ) sequence bind to streptavidin with high affinity and tend to be selected from peptide libraries panned against streptavidin [34]. As designed, this sequence was not present in the **face** library as no more than two consecutive residues were randomized to construct the library. We had anticipated that the selection protocol would result in the discovery of a novel structured motif that, perhaps, mimicked the HPQ motif in its ability to block the biotin-binding site. After four rounds of selection, five clones were picked from the enriched **face** library and the relevant portion of the plasmids sequenced. As shown in Table 5, all five clones had the same peptide sequence which, interestingly, contained the HPQ sequence. Apparently, a single A to C mutation in the codon for Asn 8 (AAT) must have been introduced during amplification in *E. coli*, producing the codon CAT that encodes histidine. An intentional Pro at position 9 and a Gln at the randomized position 10 constitute the remainder of the HPQ motif.

The portion of the plasmid encoding the peptide was sequenced for five colonies obtained after three rounds of panning and enrichment of the **loop** library. All five sequences (two were identical) contained the HPQ sequence and three of the four unique sequences followed the sequence pattern of EX<sub>2or3</sub>HPQ, where one of the additional amino acids (X) is Asp (Table 5). All four unique sequences use only one of the two possible codons for Pro, suggesting that they are sister clones that arose from rearrangement of a single progenitor sequence in *E. coli*.

#### Characterization of Streptavidin-binding Peptides

To quantitatively assess the streptavidin-binding affinity of peptides selected from the **loop** library, the peptide containing the EMQDHPQ sequence was further characterized by SPR. This complete peptide sequence was cloned from the phagemid and genetically inserted between CFP and YFP to help stabilize the stem-loop structure as well as to create a larger molecular entity to increase the SPR response. The resulting protein was designated **xxtz1/EMQDHPQ**. For the sake of comparison, a protein containing a 'linearized' version of this peptide sequence was also prepared. The linearized version, designated as **xxtz1/EMQDHPQ/Gly<sub>8</sub>**, is identical to **xxtz1/EMQDHPQ** but with the residues at positions 3, 5, 7, 9, 16, 18, 20, and 22 replaced with Gly. SPR analysis of both proteins under identical conditions showed  $K_d$ s of 320 nM and 130  $\mu$ M for **xxtz1/EMQDHPQ** and **xxtz1/EMQDHPQ/Gly<sub>8</sub>**, respectively (Supplementary Figure 2). This 400-fold decrease in  $K_d$  in going from **xxtz1/EMQDHPQ** to **xxtz1/EMQDHPQ/Gly<sub>8</sub>** indicates that the hairpin-derived portion of the putative stem-loop motif has a key role in pre-organizing the HPQ motif for binding to streptavidin. On the basis of inspection of available x-ray crystal structures of complexes between streptavidin and HPQ-containing peptides, it appears unlikely that the relatively distant Trp residues of the peptides could be involved in specific binding interactions with the protein [35]. It has previously been shown that phage display panning of randomized peptides cyclized with disulfide bonds results in the

**Table 4.** Phage display libraries

Library name	Sequence of peptide portion <sup>a</sup>
<b>Face</b>	KAW--XwXWNPX-----XGKWxwX--KNE
<b>Loop</b>	KAWTHDWTWNPgXXXXXXXXGGKWTWLRKKN

<sup>a</sup> Positions marked X were subject to saturation mutagenesis by using the codon 'NNK'.

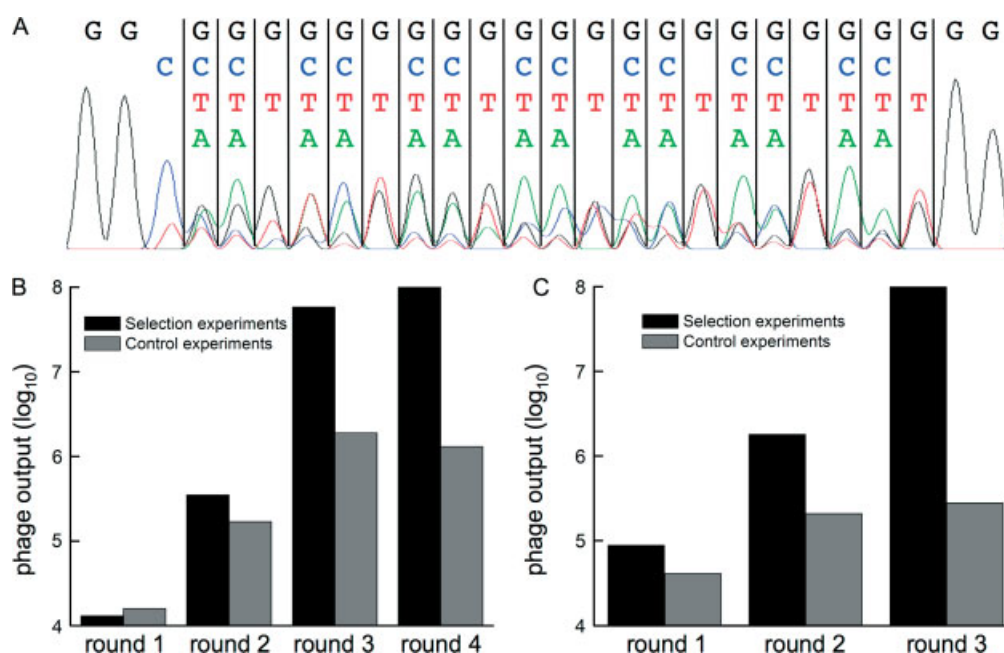


**Figure 4.** Construction and panning of phage display libraries. (A) Representative DNA sequencing data for the randomized portion of the peptide sequence (**loop** library shown). (B) Phage output for each round of selection for binding of the **face** library to streptavidin. (C) Phage output for each round of selection for binding of the **loop** library to streptavidin.

**Table 5.** Peptide sequences obtained from panning against streptavidin

library name	sequence of peptide portion <sup>a</sup>	# of occurrences
<b>face</b>	KAW- <u>PWQWHPQ</u> -----SGKWFVN--KNE	5
	gag atg cag gat cat ccg cag E M Q D H P Q	2
<b>loop</b>	gag atg gat cat ccg cag aat E M D H P Q N	1
	gag ctg gat aat cat ccg cag E L D N H P Q	1
	gag atg tcg gat cat ccg cag E M S D H P Q	1

<sup>a</sup> Randomized residue positions are in boldface type and the streptavidin-binding motif HPQ is underlined. For the **loop** library, the nucleotide and amino acid sequences of only the loop portion (XXXXXXXX in Table 4) are provided.

identification of HPQ-containing peptides with  $K_d$ s in the range of 100s of nM [36]. It has also been shown that linear HPQ-containing peptides have  $K_d$ s in the range of 100s of  $\mu$ M [37].

To further characterize the solution binding affinities of peptides selected from the **loop** library, we exploited a FRET-based binding assay. The remaining three unique peptide sequences (Table 5) were cloned into the CFP-peptide-YFP expression vector to make constructs analogous to **xxtz1/EMQDHPQ** as described in the preceding paragraph. These four proteins along with **xxtz1/EMQDHPQ/Gly<sub>8</sub>** were each incubated with varying concentrations of streptavidin and their YFP/CFP ratio determined at each concentration. Although we had expected that binding of the four copies of the CFP-peptide-YFP fusion protein to the tetrameric streptavidin would result in increased FRET efficiency due to the close proximity of multiple acceptors for each donor, the YFP/CFP ratio was observed to decrease as streptavidin concentration increased (Supplementary Figure 2). This decrease in FRET efficiency,

at concentrations of streptavidin well below the concentration of fusion protein, might be attributable to orientation effects in the crowded molecular environment of the multiple protein complex. Regardless of direction of the FRET change, the data was consistent with a two-state model in which distinct YFP/CFPs ratios were associated with both the bound and unbound states. Fitting these data to an equilibrium binding model gave  $K_d$  values of 100, 50, 80, and 90 nM for **xxtz1/EMQDHPQ**, **xxtz1/EMDHPQN**, **xxtz1/ELDNHPQ**, and **xxtz1/EMSDHPQ**, respectively. No significant change in the emission ratio was observed for **xxtz1/EMQDHPQ/Gly<sub>8</sub>** at streptavidin concentrations up to 1.5  $\mu$ M, the highest concentration tested. Given the differences in experimental protocols, the  $K_d$  values of 100 and 320 nM obtained by FRET and SPR analysis of **xxtz1/EMQDHPQ** are in reasonable agreement.

## Discussion

### FRET-based Screen for Identification of Structured Peptides

In the pursuit of a constrained peptide scaffold suitable for molecular recognition applications in the reducing environment of the cytosol, we explored the use of trpzip-type  $\beta$ -hairpin peptides. We reasoned that an exceptionally stable  $\beta$ -hairpin structure, possibly engineered by introduction of additional stabilizing interactions into an already very stable structure, may tolerate the introduction of multiple randomized amino acids and thus serve as the basis for libraries from which high affinity binding peptides could be selected by phage display. With this aim in mind, we developed a FRET-based strategy for screening large libraries of  $\beta$ -hairpin peptides to identify those that are highly folded in the cytosol of a live bacterial cell. This strategy was previously used to guide the engineering of the 20mer **xzt1**-peptide [24] from the highly folded 16mer HP5W4 [17]. In the current work, the **xzt1**-peptide has been further extended to produce the 24mer **xxtz1**-peptide. A substantial amount of time

and effort has been spent in developing [23] and exploiting [24,25] this screening strategy, and we are now in a position to reflect on its effectiveness and limitations.

It is now evident that the FRET-based screening strategy is effective for identifying peptides that are highly structured at room temperature. Highly structured peptides provide more efficient FRET between two fused fluorescent proteins than do poorly structured (or unstructured) peptides of similar length. There are three possible mechanisms by which a particular peptide sequence might produce higher FRET efficiency. The first is that, given a particular folded conformation, a higher fraction of the peptides may exist in the folded state at a given time. That is, the folding/unfolding equilibrium may lie more towards the folded structure, effectively bringing the two fluorescent proteins into closer average proximity. The second mechanism is that the peptide may simply adopt a conformation that brings the two randomly oriented fluorescent proteins into closer proximity. The third mechanism is that the peptide could adopt a structured conformation that biases the attached fluorescent proteins to a relative orientation that is favorable to FRET due to the dipole–dipole alignment (i.e.  $\kappa^2 > 2/3$ ). The important point is that all three factors require that the peptide be highly structured to explain a higher FRET efficiency.

An apparent limitation of the FRET-based screening strategy is that peptides that are selected for high FRET at room temperature do not necessarily have improved thermal stability. This conclusion is based on the fact that both **xtz1**-peptide and **xxtz1**-peptide produce substantially higher FRET efficiencies in the context of a CFP–YFP fusion protein, but the isolated peptides have equivalent or decreased thermal stability relative to **HP5W4**. This can be rationalized in terms of the second and third mechanisms mentioned above, which do not imply or require an overall improvement in thermal stability. Indeed, the overall thermal stability could be sacrificed to adopt a structured conformation that is amenable to higher FRET efficiency. For future work, it may be useful to conduct a secondary *in vitro* screen of selected FRET constructs by measuring the YFP/CFP ratio at an elevated temperature.

### Phage Display with Noncyclized $\beta$ -Hairpin Scaffolds

In contrast to the fairly extensive amount of work that has been carried out on phage display of cyclized peptides, and, of most relevance to this work, disulfide-cyclized  $\beta$ -hairpin peptides [38], relatively little effort has been invested in the development on noncyclized  $\beta$ -hairpin peptides as scaffolds for use in phage display. There are likely several contributing reasons for this discrepancy including: the relative ease of forming disulfide-cyclized peptides, a narrower range of applications in which lack of a disulfide bond would be advantageous, and (until relatively recently) a lack of highly stable candidate  $\beta$ -hairpin peptides. A growing demand for research tools for use in the reducing environment of the cytosol coupled with the advent of the trpzip-type  $\beta$ -hairpin peptides has decreased the relevance of these latter two concerns.

In this work, we explored the ability of trpzip-type  $\beta$ -hairpin peptides for the display of polypeptide libraries presented either on the highly structured face of a  $\beta$ -hairpin or as a loop inserted at the turn region. Although both presentation formats resulted in the identification of streptavidin-binding peptides containing the HPQ consensus, we have focussed our attention on characterizing the peptides isolated from the loop library. With respect to their *in vitro*

binding properties (investigated by both SPR analysis and a FRET-based solution assay), these loop peptides seem to behave similarly to previously reported covalently cyclized peptide ligands for streptavidin. Specifically, the affinities obtained for the stem–loop type structures were on par with affinities obtained with disulfide-cyclized peptide libraries [36]. Furthermore, linearizing the peptide by removing side chains that are normally critical for the fold stability of the hairpin-derived portion resulted in a 400-fold decrease in binding affinity. These characteristics provide strong support for the conclusion that the hairpin-derived portion is a key factor in dictating the binding affinity.

It is as yet unclear to us how the hairpin-derived portion of these peptides could be having such a pronounced effect on the affinity with which the loop portion binds to streptavidin. One possibility is that the **xxtz1/loop**-peptides are unfolded when in isolation, but are structurally stabilized when fused to a large protein partner such as a fluorescent protein or a phage coat protein. There is ample precedent for such behavior, as differences in properties for binding peptides genetically fused with a protein *versus* the free binding peptides have been reported for a variety of different peptide/protein combinations [39–42].

### Conclusion

In this work, we have demonstrated that noncyclized  $\beta$ -hairpin are promising candidates for use as molecular recognition scaffolds, but further engineering will be required before they become generally useful for intracellular molecular recognition applications. We found that when fused to a large solubilizing protein partner such as a fluorescent protein or a phage coat protein, the noncovalent interstrand interactions of certain  $\beta$ -hairpin peptides can act as a surrogate for cyclization in a stem–loop type peptide structure. Furthermore, phage display of these noncovalently constrained motifs can result in the identification of binding peptides with affinities that are comparable with those achieved with traditional disulfide-cyclized peptides. Peptide ligands based on these or related trpzip-derived  $\beta$ -hairpin scaffolds may one day be useful for intracellular molecular recognition applications. Although it is disappointing that the peptide structures investigated in this work were grossly destabilized by the insertion of unstructured loops, there may exist other peptide sequences that can form highly folded ‘stem–loop’ structures when free in solution.

### Supporting information

Supporting information may be found in the online version of this article.

### Acknowledgements

This research was supported by grants from NSERC and Alberta Ingenuity and was made possible with infrastructure provided by the University of Alberta and the Canadian Foundation for Innovation. We thank Cold Spring Harbor for offering their course in Phage Display of Proteins and Peptides, Carlos F. Barbas III for providing the phage display vector, and Jamie K. Scott for her critical reading of this manuscript. The authors also thank Jonathan Cartmell, Svetlana Sapelnikova, Wayne Moffat, the University of Alberta MBSU, and Mark Miskolzie of the NMR spectroscopy laboratory, for technical assistance. REC holds a Canada Research Chair in Bioanalytical Chemistry.

## References

- 1 Marasco WA. Intracellular antibodies (intrabodies) as research reagents and therapeutic molecules for gene therapy. *Immunotechnology* 1995; **1**: 1–19.
- 2 Nygren PA, Skerra A. Binding proteins from alternative scaffolds. *J. Immunol. Methods* 2004; **290**: 3–28.
- 3 Kontermann RE. Intrabodies as therapeutic agents. *Methods* 2004; **34**: 163–170.
- 4 Kohler G, Milstein C. Continuous cultures of fused cells secreting antibody of predefined specificity. *Nature* 1975; **256**: 495–497.
- 5 Winter G, Milstein C. Man-made antibodies. *Nature* 1991; **349**: 293–299.
- 6 Glockshuber R, Schmidt T, Pluckthun A. The disulfide bonds in antibody variable domains: effects on stability, folding in vitro, and functional expression in *Escherichia coli*. *Biochemistry* 1992; **31**: 1270–1279.
- 7 Bird RE, Hardman KD, Jacobson JW, Johnson S, Kaufman BM, Lee SM, Lee T, Pope SH, Riordan GS, Whitlow M. Single-chain antigen-binding proteins. *Science* 1988; **242**: 423–426.
- 8 Proba K, Worn A, Honegger A, Pluckthun A. Antibody scFv fragments without disulfide bonds made by molecular evolution. *J. Mol. Biol.* 1998; **275**: 245–253.
- 9 Ohage E, Steipe B. Intrabody construction and expression. I. The critical role of VL domain stability. *J. Mol. Biol.* 1999; **291**: 1119–1128.
- 10 Binz HK, Amstutz P, Pluckthun A. Engineering novel binding proteins from nonimmunoglobulin domains. *Nat. Biotechnol.* 2005; **23**: 1257–1268.
- 11 Hosse RJ, Rothe A, Power BE. A new generation of protein display scaffolds for molecular recognition. *Protein Sci.* 2006; **15**: 14–27.
- 12 Skerra A. Engineered protein scaffolds for molecular recognition. *J. Mol. Recognit.* 2000; **13**: 167–187.
- 13 Bianchi E, Folgori A, Wallace A, Nicotra M, Acali S, Phalipon A, Barbato G, Bazzo R, Cortese R, Felici F, Pessi A. A conformationally homogeneous combinatorial peptide library. *J. Mol. Biol.* 1995; **247**: 154–160.
- 14 Klug A. Zinc finger peptides for the regulation of gene expression. *J. Mol. Biol.* 1999; **293**: 215–218.
- 15 Herman RE, Badders D, Fuller M, Makienko EG, Houston MEJ, Quay SC, Johnson PH. The Trp cage motif as a scaffold for the display of a randomized peptide library on bacteriophage T7. *J. Biol. Chem.* 2007; **282**: 9813–9824.
- 16 Cochran AG, Skelton NJ, Starovasnik MA. Tryptophan zippers: stable, monomeric beta-hairpins. *Proc. Natl. Acad. Sci. U.S.A.* 2001; **98**: 5578–5583.
- 17 Fesinmeyer RM, Hudson FM, Andersen NH. Enhanced hairpin stability through loop design: the case of the protein G B1 domain hairpin. *J. Am. Chem. Soc.* 2004; **126**: 7238–7243.
- 18 Gururaja TL, Narasimhamurthy S, Payan DG, Anderson DC. A novel artificial loop scaffold for the noncovalent constraint of peptides. *Chem. Biol.* 2000; **7**: 515–527.
- 19 Marks KM, Rosinov M, Nolan GP. In vivo targeting of organic calcium sensors via genetically selected peptides. *Chem. Biol.* 2004; **11**: 347–356.
- 20 Bodenmuller H, Schilling E, Zachmann B, Schaller HC. The neuropeptide head activator loses its biological activity by dimerization. *EMBO J.* 1986; **5**: 1825–1829.
- 21 Lai JR, Gellman SH. Reinvestigation of the proposed folding and self-association of the neuropeptide head activator. *Protein Sci.* 2003; **12**: 560–566.
- 22 Gururaja TL, Payan DG, Anderson DC. Gas phase dimerization of neuropeptide head activator analogs useful for the noncovalent constraint of peptides. *Biopolymers* 2007; **88**: 55–63.
- 23 Cheng Z, Campbell RE. Assessing the structural stability of designed beta-hairpin peptides in the cytoplasm of live cells. *Chembiochem* 2006; **7**: 1147–1150.
- 24 Cheng Z, Miskolzie M, Campbell RE. In vivo screening identifies a highly folded beta-hairpin peptide with a structured extension. *Chembiochem* 2007; **8**: 880–883.
- 25 Cheng Z, Campbell RE. Fluorescence-based characterization of genetically encoded peptides that fold in live cells: progress toward a generic hairpin scaffold. *Proc. SPIE* 2007; **6449**: 64490S.
- 26 Scott JK, Smith GP. Searching for peptide ligands with an epitope library. *Science* 1990; **249**: 386–390.
- 27 Zacharias DA, Violin JD, Newton AC, Tsien RY. Partitioning of lipid-modified monomeric GFPs into membrane microdomains of live cells. *Science* 2002; **296**: 913–916.
- 28 Griesbeck O, Baird GS, Campbell RE, Zacharias DA, Tsien RY. Reducing the environmental sensitivity of yellow fluorescent protein. Mechanism and applications. *J. Biol. Chem.* 2001; **276**: 29188–29194.
- 29 Rizzo MA, Springer GH, Granada B, Piston DW. An improved cyan fluorescent protein variant useful for FRET. *Nat. Biotechnol.* 2004; **22**: 445–449.
- 30 Hochuli E, Bannwarth W, Dobei H, Gentz R, Stuber D. Genetic approach to facilitate purification of recombinant proteins with a novel metal chelate adsorbent. *Bio-Technology* 1988; **6**: 1321–1325.
- 31 Barbas III CF, Burton D, Scott JK, Silverman GJ. *Phage Display: A Laboratory Manual*. Cold Spring Harbor Laboratory Press: Cold Spring Harbor, NY, 2001.
- 32 Tatko CD, Waters ML. The geometry and efficacy of cation-pi interactions in a diagonal position of a designed beta-hairpin. *Protein Sci.* 2003; **12**: 2443–2452.
- 33 Grishina IB, Woody RW. Contributions of tryptophan side chains to the circular dichroism of globular proteins: exciton couplets and coupled oscillators. *Faraday Discuss.* 1994; **99**: 245–262.
- 34 Devlin JJ, Panganiban LC, Devlin PE. Random peptide libraries: a source of specific protein binding molecules. *Science* 1990; **249**: 404–406.
- 35 Katz BA. Binding to protein targets of peptidic leads discovered by phage display: crystal structures of streptavidin-bound linear and cyclic peptide ligands containing the HPQ sequence. *Biochemistry* 1995; **34**: 15421–15429.
- 36 Giebel LB, Cass R, Milligan DL, Young D, Arze R, Johnson C. Screening of cyclic peptide phage libraries identifies ligands that bind streptavidin with high affinities. *Biochemistry* 1995; **34**: 15430–15435.
- 37 Weber PC, Pantoliano MW, Thompson LD. Crystal structure and ligand binding studies of a screened peptide complexed with streptavidin. *Biochemistry* 1992; **31**: 9350–9354.
- 38 Uchiyama F, Tanaka Y, Minari Y, Tokui N. Designing scaffolds of peptides for phage display libraries. *J. Biosci. Bioeng.* 2005; **99**: 448–456.
- 39 Jouault T, Fradin C, Dzierzinski F, Borg-Von-Zepelin M, Tomavo S, Corman R, Trinel PA, Kerckaert JP, Poulain D. Peptides that mimic *Candida albicans*-derived  $\beta$ -1,2-linked mannosides. *Glycobiology* 2001; **11**: 693–701.
- 40 Menendez A, Chow KC, Pan OC, Scott JK. Human immunodeficiency virus type 1-neutralizing monoclonal antibody 2F5 is multispecific for sequences flanking the DKW core epitope. *J. Mol. Biol.* 2004; **338**: 311–327.
- 41 Saphire EO, Montero M, Menendez A, van Houten NE, Irving MB, Pantophlet R, Zwick MB, Parren PW, Burton DR, Scott JK, Wilson IA. Structure of a high-affinity “mimotope” peptide bound to HIV-1-neutralizing antibody b12 explains its inability to elicit gp120 cross-reactive antibodies. *J. Mol. Biol.* 2007; **369**: 696–709.
- 42 Menendez A, Calarese DA, Stanfield RL, Chow KC, Scanlan CN, Kunert R, Katinger H, Burton DR, Wilson IA, Scott JK. A peptide inhibitor of HIV-1 neutralizing antibody 2G12 is not a structural mimic of the natural carbohydrate epitope on gp120. *FASEB J.* 2008; **22**: 1380–1392.